Available online at www.sciencedirect.com
SCIENCE DIRECT
Journal of Catalysis 239 (2006) 227–236
JOURNAL OF CATALYSIS
www.elsevier.com/locate/jcat

The origin of rhodium promotion of Fe_3O_4–Cr_2O_3 catalysts for the high-temperature water–gas shift reaction

Yun Lei, Noel W. Cant, David L. Trimm *

School of Chemical Engineering and Industrial Chemistry, The University of New South Wales, Sydney, NSW 2052, Australia

Received 23 November 2005; revised 24 January 2006; accepted 25 January 2006

Abstract

Rhodium promotion of iron–chromium oxide (Fe–Cr) catalysts for the water–gas shift (WGS) reaction was investigated through measurement of the rates of individual reduction and reoxidation steps. The temperature-programmed reduction of the starting Fe_2O_3 form by H_2 is accelerated by rhodium, with the extent of oxygen removal at 450 °C corresponding to Fe_3O_4 formation. The corresponding reduction by CO proceeds further, in agreement with bulk thermodynamic expectations. However, rhodium has no effect on the oxygen removal rate, although it leads to substantially increased carbon deposition. The behavior with respect to reoxidation of reduced catalysts is somewhat similar. Rhodium greatly enhances H_2 release during reoxidation by water, presumably by recombining hydrogen atoms transferred from oxide to metal by reverse spillover. The rate of H_2 evolution from the Rh/Fe–Cr system at 280 °C is greater than that from Fe–Cr at 380 °C. Reoxidation by CO_2 is not promoted by Rh and is much slower than that by H_2O for the Rh-containing catalyst. Likewise, reoxidation by H_2O/CO_2 mixtures results in a much higher yield of H_2 relative to CO for the promoted catalyst compared with the unpromoted one. The extent to which catalysts previously equilibrated in WGS feeds at 350 °C can then be reduced in pulses of CO or H_2 depends on the composition of the WGS feed. Fe–Cr catalysts do not reduce in H_2 after exposure to H_2O/CO (2:1) or a reformate ($H_2O/CO/H_2/CO_2$) feed. Hydrogen reduction is possible with Rh/Fe–Cr after exposure to H_2O/CO but not after exposure to reformate, for which thermodynamic considerations suggest that the working oxidation state may be lower. The greater reducing power of CO leads to continuing reduction after treatment with both prior feeds. Overall, it is concluded that of the two steps that may restrict the rate of the WGS reaction over iron–chromium oxide catalysts (reduction by CO and H_2 generation through reoxidation by water), rhodium acts primarily by accelerating the second.

Keywords: Water–gas shift reaction; Iron–chromium oxides; Rhodium promotion; Mechanism

1. Introduction

Interest in the development of small-scale systems for the conversion of natural gas or liquid hydrocarbons to hydrogen for use in PEM fuel cells in vehicles and at service stations has sparked renewed interest in catalysts capable of lowering carbon monoxide content via the water–gas shift (WGS) equilibrium [1,2],

$$CO + H_2O = CO_2 + H_2, \quad \Delta H = -41.1\ \text{kJ/mol}. \tag{1}$$

Most attention has been focused on systems with activity comparable to known copper–zinc oxide catalysts but with greater stability toward water and air during intermittent use [3,4]. Combinations of gold and ceria show considerable promise and are stable to 300 °C [5], but long-term operation at higher temperatures has yet to be established. An upstream catalyst with sufficient activity to achieve equilibrium with high flow rates at the maximum tolerable operational temperature may then be desirable. Conventional high-temperature-shift catalysts based on oxides of iron and chromium are well established industrially [6], but further promotion is desirable [7]. We have recently found that small amounts of rhodium can increase the activity by a factor of four [8,9], and the present study is directed at the origin of this promotion.

As discussed by Keiski et al. [10], iron oxide–chromium oxide WGS catalysts appear to operate by a mechanism that includes adsorptive and redox steps, for example,

* Corresponding author.
E-mail addresses: david.trimm@csiro.au, d.trimm@unsw.edu.au (D.L. Trimm).

0021-9517/$ – see front matter
doi:10.1016/j.jcat.2006.01.033

$$CO + O(s) \rightarrow CO_2(s), \quad (2)$$

$$CO_2(s) \rightarrow CO_2 + *, \quad (3)$$

$$H_2O + * \rightarrow H_2O(s), \quad (4)$$

$$H_2O(s) + O(s) \rightarrow 2OH(s), \quad (5)$$

$$2\,OH(s) \rightarrow 2O(s) + H_2, \quad (6)$$

where * represents a surface vacancy and (s) represents a surface species. Transient isotope experiments indicate that the first step (reduction by CO) or the final step (hydrogen release) can be rate-limiting [11–13]. Thus it is reasonable to think that rhodium promotes one or the other of these steps.

The relatively facile reversibility of WGS complicates the understanding of the reaction mechanism and the application of surface analytical techniques. However, reduction of iron oxide–chromium oxides is potentially subject to bulk thermodynamic constraints. The chromia is generally considered a structural promoter in the system [14,15], and XPS studies show that the Cr valence state is the same after exposure to CO/H_2O, H_2, and 2% O_2 feeds [16]. Thus redox processes, under working conditions, can be considered in terms of iron compounds alone.

The stable oxide in equilibrium with WGS feeds is Fe_3O_4, magnetite [6]. The next lower oxide (wüstite, nonstoichiometric Fe_xO, $x \sim 0.947$) is thermodynamically unstable with respect to disproportionation to Fe_3O_4 and Fe below ∼570 °C [17]. In this case, reduction of Fe_3O_4 in H_2 or CO at lower temperatures is expected to proceed directly to Fe, as is the case during the reduction of ammonia synthesis catalysts based on fused magnetite precursors [6,18], even though the redox process may proceed formally via FeO [19]. FeO(111) is known to be a surface phase of both Fe_3O_4 and Fe_2O_3 when they are formed as thin films [20]. X-ray diffraction (XRD) measurements show that temperature-programmed reduction (TPR) of Fe_2O_3 in 10% H_2/Ar to 500 °C (i.e., below the wüstite stability limit) occurs with partial conversion of Fe_3O_4 to a FeO phase between 360 and 500 °C [21]. Reduction to Fe requires pure H_2; however, it is possible to render wüstite stable for long periods at 400 °C by the inclusion of calcium [22].

In the present work we compared of the rates of reduction (by CO and H_2) and reoxidation (by CO_2 and H_2O) of unpromoted and rhodium-promoted WGS catalysts using the dynamic technique of pulse injection and step changes in concentration. The results shed light on the likely mechanism for rhodium promotion of the WGS reaction.

2. Experimental

Pulse experiments were carried out using a modified version of the flow system used previously for activity and kinetic determinations [8,9]. The system uses mass flow controllers for the delivery of gases, a high-precision syringe pump (ISCO LC-260D), and a heated vaporizer for water with two gas chromatographs for analysis of CO, CO_2, and H_2. In the pulse experiments, the sample of catalyst is allowed to reach a steady state through reaction in either a standard reaction mixture (10% CO, 20% H_2O, balance N_2) or a synthetic reformate feed (7% CO, 8% CO_2, 22% H_2O, 37% H_2, balance N_2) for some hours at 350 °C. It is then flushed with either He (when CO pulses are to be tested) or Ar (with H_2). Pulses of pure CO or H_2 are then introduced by switching a six-port valve fitted with a 0.5-mL loop. The stream leaving the reactor bypasses the gas chromatograph analysis system and passes to a separate thermal conductivity detector (TCD) via a U-tube trap cooled in liquid nitrogen. The trap serves to eliminate interference from product water when H_2 is fed and to trap CO_2 when pulsing CO. Once analysis of CO is complete, the CO_2 collected is vaporized by replacing the liquid nitrogen by warm water and analyzed with the TCD.

The TPR and step-change experiments were carried out in a second system fitted with a quadrupole mass spectrometer (Balzers Thermostar GSD 301T) operated in multiple-ion monitoring mode. The system comprises a set of Valco four-port valves that allow rapid switching between two streams, one containing He alone and the other containing one or more reactants in 1% Ar/He. The argon serves as marker for the commencement of exposure and as a check on any drift in the baseline or sensitivity of the mass spectrometer during the course of a day. The reactant(s)/Ar/He feed was analyzed on bypass before and after each exposure, and the Ar signal ($m/z = 40$) was used to normalize the signals at the other m/z values logged onto the computer. This system uses a saturator at ∼20 °C for the delivery of water, which limits the H_2O partial pressure to 2% of the atmosphere absolute pressure at which the reactor is operated.

Catalysts were prepared as described previously [8,9] by first precipitating $Fe(OH)_3$ from iron nitrate using 30% ammonium hydroxide to a pH of 7.5–8.0. The precipitate was filtered and washed and then converted to thick slurry. Chromium nitrate solution was stirred into the slurry (pH 7.5–8.0), and the mixture was aged for 8 h. After further filtration and washing, the solid was dried (110 °C for 16 h) and calcined in air (500 °C for 3 h). Rhodium was introduced by impregnation of a 150–250 μm fraction of the calcined Fe_2O_3–Cr_2O_3 with rhodium nitrate using the incipient wetness technique, followed by further drying and calcination as above.

Inductively coupled plasma (ICP) analysis showed that the catalyst contained 0.97 wt% Rh; XRF found 91.5% Fe_2O_3 and 7.36% Cr_2O_3 (residual trapped Na_2O). The surface area measured by the BET method was found to be 46 m^2/g. The metal surface area was too low to measure.

Oxidized and reduced catalysts were also examined using a Philips X'Pert XRD system fitted with a Ni-filtered Cu-K_α radiation source and an ESCALAB 220i-XL XPS instrument fitted with a monochromated Al-K_α source. Reduction was carried out in 6% H_2/He as for the experiments described in Section 3.3 on a temperature ramp ending at 400 °C. The XRD samples, both calcined and reduced, were exposed to air during the measurements. The XPS samples were exposed briefly during transfer to the instrument.

Based on the bulk analysis (XRF and ICP), the atomic ratio was found to be Fe:Cr:Rh = 1:0.08:0.008. The corresponding ratios obtained by XPS were Fe:Cr:Rh = 1:0.30:0.08 for the

calcined catalyst and Fe:Cr:Rh = 1:0.29:0.058 for the reduced sample. It is clear that both Rh and Cr were concentrated at the surface. Reduction was accompanied by the conversion of largely Rh_2O_3 to metallic Rh and of Cr(VI) to Cr(III). Iron was reduced from Fe(III) to a mixture of Fe(II) and Fe(III), as would be expected for the formation of magnetite (Fe_3O_4). The apparent amount of Rh on the surface was somewhat less after reduction, but this would be expected for the conversion of an oxidic layer to more compact Rh crystallites, thereby exposing more of the underlying support.

The XRD measurements of calcined samples showed strong lines due to hematite (Fe_2O_3) alone. Reduction showed complete conversion to magnetite in the unpromoted sample, with some evidence of further slight reduction in the promoted sample. No Rh lines were detectable, as would be expected were the Rh highly dispersed.

Comparison measurements between unpromoted and promoted catalysts were carried out using samples of mass ∼50 mg mounted between quartz wool plugs in a stainless steel tube (pulse experiments) or a Pyrex glass U-tube (step-change system). The various pretreatments used before exposure to reductants and reactants are described below.

Comparisons of the catalytic activity of the unpromoted and promoted catalysts with a commercial WGS catalyst were carried out using a feed comprising 9% H_2O, 9% CO, and balance N_2. All catalysts were calcined in air (500 °C for 5 h) and prereduced in a stream of 10% H_2 in N_2 at 400 °C for 2 h. The catalysts were then exposed to the WGS feed and allowed to reach steady activity at each temperature (∼2 h), after which measurements were taken.

3. Results and discussion

3.1. Catalytic activities

The promoting effect of rhodium for the high-temperature iron–chromium oxide WGS catalyst has been reported previously [8,9]. Some measure of the advantage to be gained is provided in Table 1, which compares activities per gram at temperatures from 350 to 500 °C. The rhodium promoted sample is almost five times more active as the unpromoted one at 350 °C and 1.5 times more active at 500 °C. The rate advantage over the commercial high-temperature WGS catalyst (a current-generation copper-promoted iron–chromium oxide system) is slightly greater.

Table 1
Activity comparison for WGS reaction with H_2O/CO feed[a]

Catalyst	10^5 × reaction rate ($mol_{CO}/(g\,s)$)			
	350 °C	400 °C	450 °C	500 °C
Fe_3O_4–Cr_2O_3	2.0	5.9	12.4	19.5
1 wt% Rh/Fe_3O_4–Cr_2O_3	9.9	16.5	24.2	30.8
Commercial catalyst	2.0	4.2	9.7	16.6

[a] 9% H_2O, 9% CO, balance N_2.

3.2. Thermodynamic considerations

Although both the WGS reaction and pulse/step studies were carried out in a dynamic mode, thermodynamic considerations can provide some guidance as to what can be expected. The reduction of bulk Fe_2O_3 to Fe_3O_4 is highly favorable using both H_2 and CO, as shown in Fig. 1. The phase diagram in Fig. 1A, calculated from the data of Barin [23], shows the system Fe_2O_3/Fe_3O_4/$Fe_{0.947}O$(wüstite)/Fe in terms of the CO_2/CO ratio at which phase interconversion will occur at equilibrium. In the case of the H_2O/CO and reformate input feeds, the CO_2/CO ratios shown correspond to values that would be reached were the WGS reaction at equilibrium. Likewise, the data for the H_2O/H_2 feed is plotted in terms of the CO_2/CO ratios that provide equivalent reducing power.

At 450 °C (the maximum temperature used here), Fe_2O_3 can convert to Fe_3O_4 when $\ln(CO_2/CO)$ is <13.5 (i.e., $CO_2/CO \approx 7 \times 10^5$, which would allow >99.99% conversion starting from CO were a thermodynamically limited reduction to proceed). Further reduction direct to Fe becomes feasible at 450 °C when $\ln(CO_2/CO)$ is <0.17 (a CO_2/CO ratio of ∼1.2 and potential CO conversion of 53%). Reduction to $Fe_{0.947}O$ is not expected at this temperature, because wüstite is unstable below ∼570 °C. The line with solid symbols in Fig. 1A corresponds to the H_2O/H_2 ratio at which Fe_3O_4 can convert to Fe at 450 °C. This ratio is 0.17, representing a potential H_2 conversion of ∼15%.

Standard thermodynamic tabulations, such as those of Barin [23], commonly contain data for another undefined iron oxide designated simply as FeO. The phase diagram based on data for this substance is shown in Fig. 1B. Here "FeO" is able to form as an intermediate during reduction of Fe_3O_4 at 450 °C when $\ln(CO_2/CO)$ is <2.7 (equivalent to a CO_2/CO ratio of 15 with a potential CO conversion of 94%) and can undergo further reduction to Fe when $\ln(CO_2/CO)$ is < -0.17 (ratio 0.84; 46% conversion). The corresponding ratios for the H_2O/H_2 couple are 2.2 (allowing 69% H_2 conversion) and 0.08 (allowing 7% conversion), respectively.

Bulk thermodynamic considerations such as these are probably not applicable during temperature programming when reduction is kinetically controlled, especially for amorphous material with a relatively high surface-to-volume ratio. However, they can provide some guidance as to what might form under isothermal conditions when exposure times are long.

3.3. TPR and reoxidation

Initial experiments were carried out using calcined material to provide an indication of the effect of Rh on reduction and reoxidation as a prelude to testing of samples treated under WGS reaction conditions. Results for the TPR of the starting mixed Fe_2O_3–Cr_2O_3 oxides, previously calcined in air, carried out in a stream containing 6.4% H_2 in He are shown in Fig. 2. The temperature giving the maximum rate of H_2 consumption is considerably lower for the Rh-promoted material (350 °C) than for the unpromoted solid (400 °C). Thus Rh facilitates reduction, presumably through H_2 dissociation and spillover to the

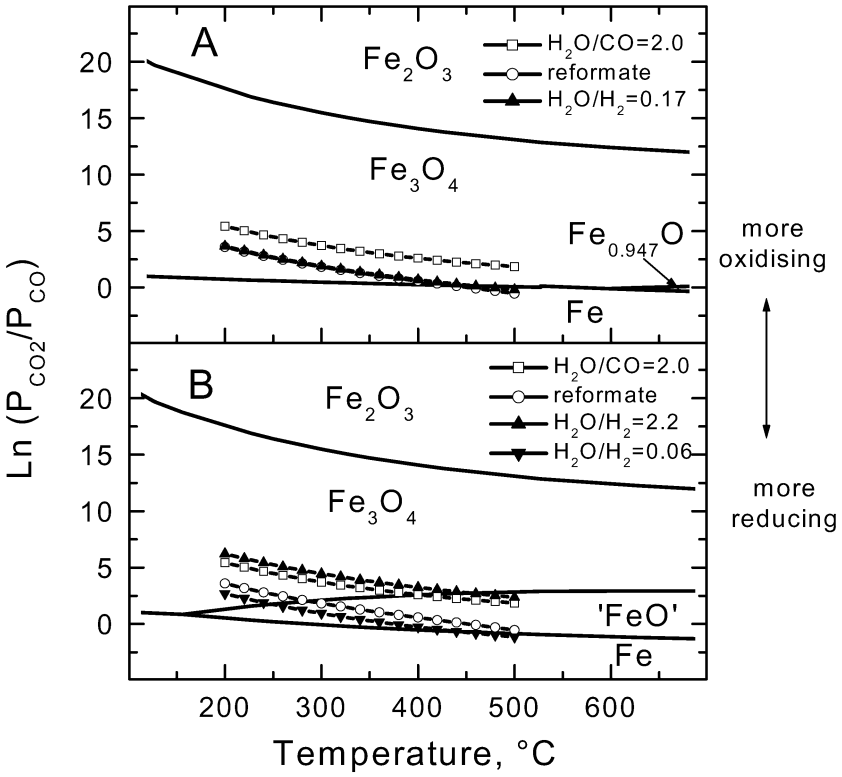

Fig. 1. Bulk phase diagrams calculated from the data in Ref. [23]. (A) The Fe_2O_3/Fe_3O_4/wüstite ($FeO_{0.947}$)/Fe system; (B) The Fe_2O_3/Fe_3O_4/'FeO'/Fe system. The points for reformate (7% CO, 8% CO_2, 22% H_2O, 37% H_2, balance N_2) in A underlie those for $H_2O/H_2 = 0.17$.

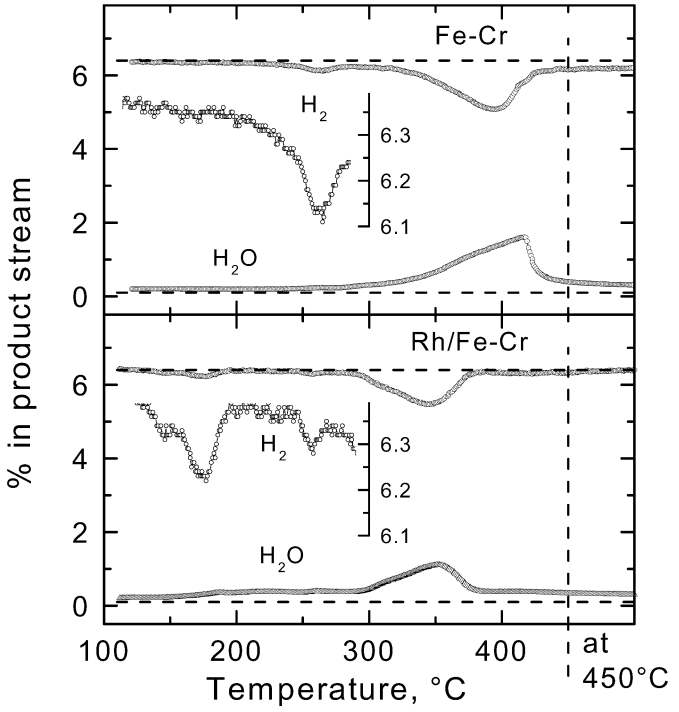

Fig. 2. Temperature-programmed reduction of ~50 mg samples of Fe–Cr and Rh/Fe–Cr in 6.4% H_2/He flowing at ~25 cm^3/min. The ramp rate was ~7 °C/min.

oxide. The extent of oxygen removal relative to the number of O^{2-} ions initially present in Fe_2O_3 is ~0.1 (Table 2). This is in line with the stoichiometric ratio of 1:9 (= 0.11) expected for

Table 2
Oxygen removal during temperature-programmed reduction in hydrogen

	O atoms removed relative to those present in starting Fe_2O_3				
	130–200 °C	200–280 °C	280–450 °C	At 450 °C	Total
Fe–Cr	<0.001	0.008	0.097	0.001	0.10
Rh/Fe–Cr	0.007	0.004	0.098	0.005	0.11

$$3Fe_2O_3 + H_2 \rightarrow 2Fe_3O_4 + H_2O. \quad (7)$$

However it is impossible to rule out nonuniform reduction with the surface reduced to a greater extent than the bulk.

Considering the foregoing phase diagrams, further reduction of Fe_3O_4 to Fe or "FeO" is feasible. The extent to which H_2 can be consumed is limited by water formation and the consequent H_2O:H_2 ratio. Up to 15% of the H_2 can be consumed for a reduction to Fe (from Fig. 1A); up to 69%, for a reduction to "FeO" (from Fig. 1B). Drifts in baseline make it impossible to exclude the possibility of some further reduction when the Fe–Cr sample is held at 450 °C or when the Rh/Fe–Cr sample is heated above 380 °C.

The expanded inset plots in Fig. 2 show a second difference between the systems. The Rh-promoted catalyst exhibits a small peak at 180 °C and an even smaller one near 260 °C. Only the second peak is evident for the unpromoted oxide, with a peak area qualitatively equal to the two peaks seen with Rh/Fe–Cr. These peaks may arise through reduction of oxygen at the surface of Fe_2O_3 or possibly associated with the surface Cr(VI) ions observed by XPS, with the lower-temperature peak arising from reduction of ions close to Rh particles and the other

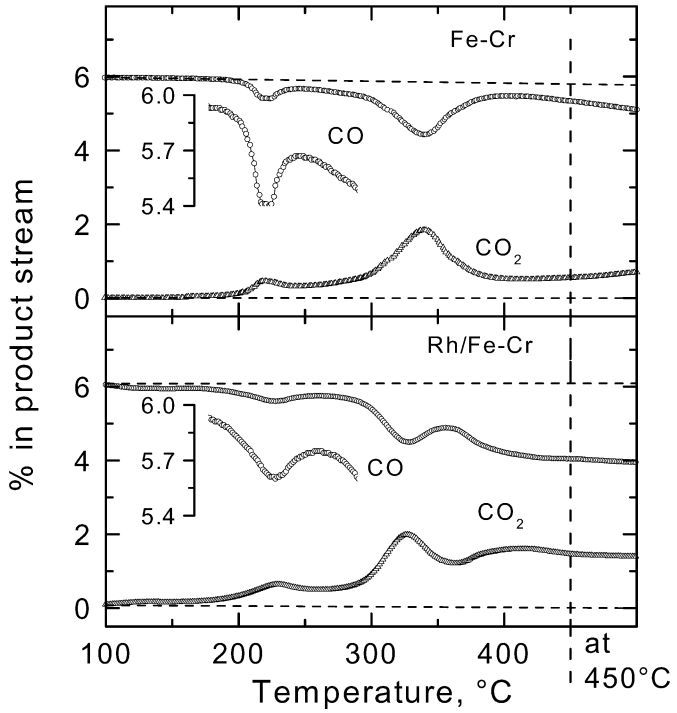

Fig. 3. Temperature-programmed reduction of ∼50 mg samples of Fe–Cr and Rh/Fe–Cr in 6.0% CO/He flowing at ∼25 cm^3/min. The ramp rate was ∼9 °C/min.

peak arising from ions at positions on the oxide surface that are too remote from Rh to benefit from hydrogen spillover. Integration of these low-temperature peaks is difficult because of their small size, but their combined amount, expressed in terms of O atoms removed relative to surface O^{2-} ions (calculated assuming 1.2×10^{19} ions/m^2), is approximately 0.14, again in reasonable agreement with the 1:9 stoichiometry derived from Eq. (7).

As noted in Section 2, XRD examination showed the complete loss of hematite lines after reduction of both the promoted and unpromoted samples. Magnetite was the predominant product, but the reduced unpromoted sample showed very weak lines attributable to trace amounts of FeO. XRD examination of the Rh-promoted sample showed small but significant amounts of metallic iron with no evidence of FeO. The characteristics of TPR using CO were somewhat different (Fig. 3). Both catalysts exhibited a single small low-temperature reduction peak at the same position (close to 225 °C, lower than that for reduction of the unpromoted catalyst with H_2) and a larger peak at 335 °C (lower than that for either catalyst when using H_2). Thus, unlike the case with H_2, Rh does not facilitate reduction by CO. However, it is clear that the Rh-promoted sample consumed much more CO at temperatures above 360 °C and that the ratio of CO_2 produced to CO reacted eventually fell below 0.8, inferring that some CO was being consumed without formation of CO_2. This could arise either through production of iron carbide, for example,

$$Fe_3O_4 + 6CO \rightarrow Fe_3C + 5CO_2, \quad (8)$$

or through a combination of further reduction of Fe_3O_4 to Fe (or perhaps 'FeO') and the rhodium-facilitated Boudouard reaction,

$$2CO \rightarrow CO_2 + C(s). \quad (9)$$

Both reactions are thermodynamically feasible, but the latter seems more likely, because the CO_2/CO ratio was not constant and at some temperatures fell below the 0.83 expected from the stoichiometry of Eq. (8).

Note that the CO consumption that gave rise to the low-temperature peak at 225 °C was considerably greater than the corresponding peak(s) with hydrogen. The ratio of oxygen atoms removed to surface O^{2-} ions was ∼0.6, implying either that reduction in the surface layer went beyond the 1:9 ratio corresponding to the Fe_2O_3-to-Fe_3O_4 transformation or that the reduction was not confined to the surface at this temperature. The ratio of 0.6 is between those expected for reduction of the surface to Fe (a ratio of 1.0) and to FeO (0.33).

Table 3
Oxygen removed and carbon deposited during CO-TPR

	O atoms removed relative to those present in starting Fe_2O_3				
	180–270 °C	270–390 °C	390–450 °C	At 450 °C	Total
Fe–Cr					
O removed[a]	0.02	0.14	0.04	0.08	0.28
C deposited[b]	0.00	0.00	0.00	0.02	0.02
Rh/Fe–Cr					
O removed[a]	0.04	0.16	0.06	0.03	0.29
C deposited[b]	0.00	0.00	0.05	0.09	0.15

[a] Calculated using 2 × CO_2 (formed) − CO (consumed).
[b] Calculated using CO (consumed) − CO_2 (formed).

Table 3 compares the two catalysts in terms of oxygen removal and carbon deposition calculated from the CO consumed and the CO_2 produced. Carbon deposition on the Fe–Cr system was negligible compared with that on Rh/Fe–Cr. The extent of oxygen removal (∼28% of that originally present) was similar for the two systems and almost three times greater than that found when using H_2 (Table 2). Thus TPR in CO reduced the samples substantially below Fe_3O_4. This is in line with its greater reducing power, which, according to the earlier considerations, allowed up to 53% utilization of CO during conversion of Fe_3O_4 to Fe (Fig. 1A) compared with 15% for the same reaction with H_2.

The amounts of carbon formed were also determined by temperature-programmed reoxidation in O_2, as shown in Fig. 4. Both catalysts gave rise to a low-temperature peak of O_2 consumption at ∼190 °C and further reoxidation above 300 °C. The second stage was accompanied by CO_2 formation, small for Fe–Cr but larger and continuing much longer for Rh/Fe–Cr. Estimated quantities of carbon removed from the samples, and of oxygen restored to them during reoxidation, are summarized in Table 4. The agreement with the corresponding data calculated for TPR in CO (Table 3) is reasonable, bearing in mind that most of the calculations involve differences, many between quite similar quantities.

3.4. Reoxidation in water and carbon dioxide

These experiments were carried out with repeatedly used samples that were pretreated between tests similar to those sam-

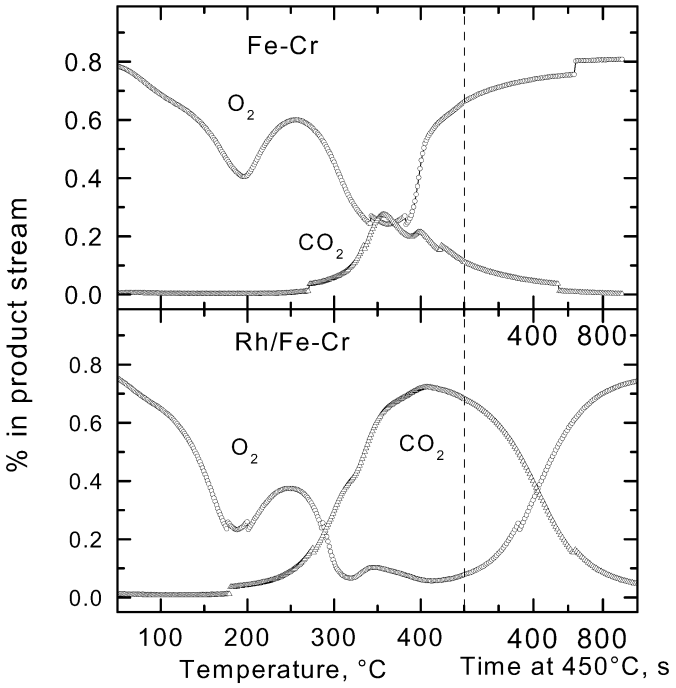

Fig. 4. Temperature-programmed reoxidation of ∼50 mg samples of Fe–Cr and Rh/Fe–Cr previously reduced in 6% CO/He (as per Fig. 2) in 0.8% O_2/He flowing at ∼25 cm^3/min.

Table 4
Oxygen deposited and carbon removed during TPO in oxygen of CO reduced catalysts

	O atoms removed relative to those present in starting Fe_2O_3			
	180–270 °C	270–390 °C	390–450 °C	Total
Fe–Cr				
O deposited[a]	0.11	0.13	0.01	0.25
C removed[b]	0.00	0.03	0.01	0.04
Rh/Fe–Cr				
O deposited[a]	0.16	0.13	0.03	0.32
C removed[b]	0.01	0.12	0.04	0.17

[a] Calculated using 2 × {O_2 (consumed) − CO_2 (formed)}.
[b] Calculated from CO_2 (formed).

ples used in our catalytic studies [8]. This pretreatment comprised heating the samples up to 400 °C in 6.4% H_2/He over 1 h and keeping them at this temperature for 2 h before flushing with helium alone. Subsequent exposure to water (2.0% H_2O/He) led to the evolution of hydrogen (Fig. 5). The Rh-promoted sample showed nearly complete conversion of H_2O to H_2 for a period of several hundred seconds at 380 and 330 °C. Significant reaction occurred even at 150 °C. Reoxidation was much less extensive with the Fe–Cr sample. Clearly, Rh greatly promoted H_2 generation, presumably by providing sites that can combine hydrogen atoms derived from hydroxyl groups to liberate H_2 according to reaction (6).

Results for reoxidation of hydrogen-reduced samples in 2.2% CO_2/He are shown in Fig. 6. The Rh-promoted sample reoxidized much more slowly than the sample in H_2O/He, demonstrating similar behavior as the unpromoted sample. If anything, the amount of CO generated initially was less when

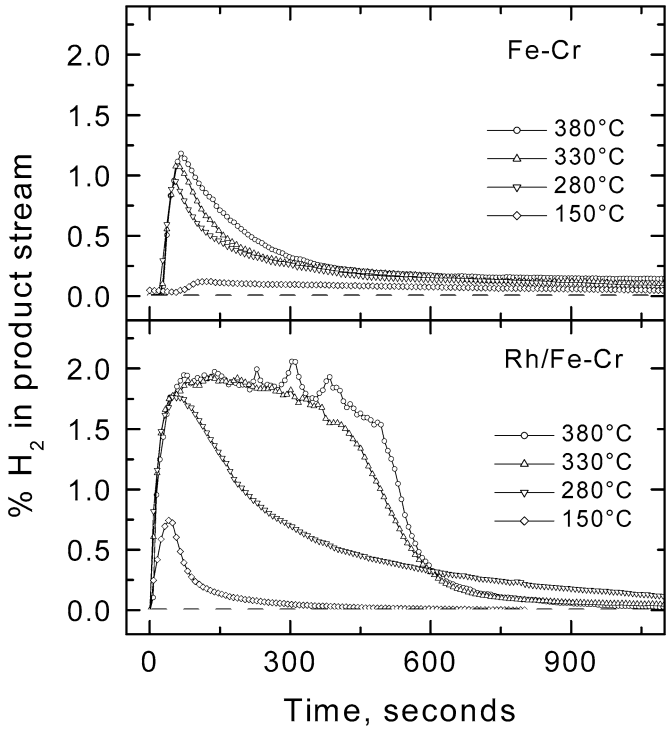

Fig. 5. Reoxidation of ∼50 mg samples of Fe–Cr and Rh/Fe–Cr, previously reduced in 6% H_2/He, in ∼2.0% H_2O/He flowing at ∼22 cm^3/min.

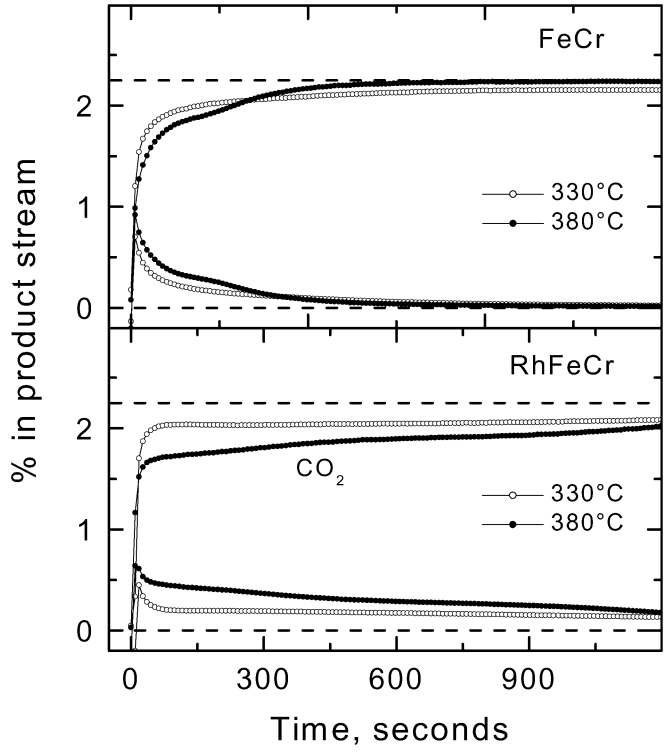

Fig. 6. Reoxidation of ∼50 mg samples of Fe–Cr and Rh/Fe–Cr, previously reduced in 6% H_2/He, in ∼2.2% CO_2/He flowing at ∼26 cm^3/min.

Rh was present, probably reflecting adsorption and/or dissociation with carbon formation. Consumption of CO_2 with some CO formation continued at a low level with the Rh sample in a way not evident for Fe–Cr but that is difficult to quantify with

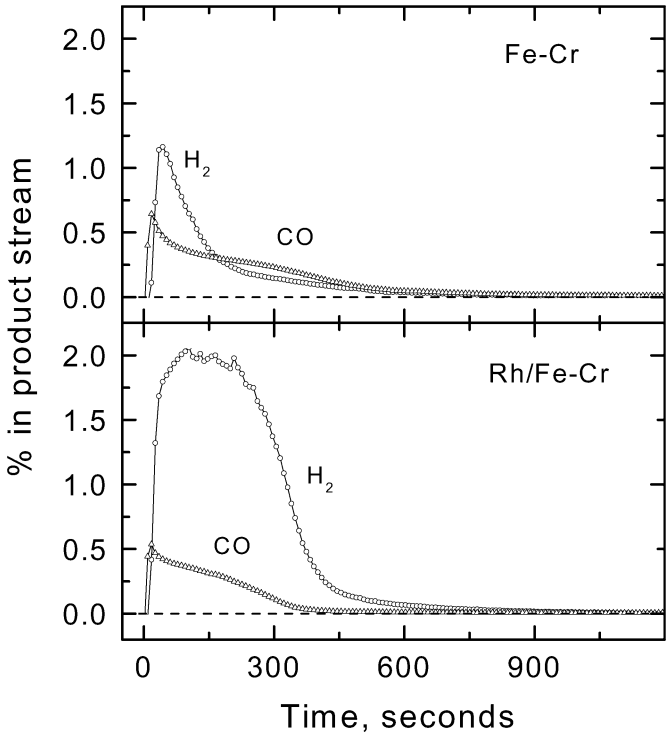

Fig. 7. Reoxidation of ∼50 mg samples of Fe–Cr and Rh/Fe–Cr, previously reduced in 6% H_2/He, in ∼2.0% H_2O/2.2% CO_2/He mixture at 380 °C. The total flow rate was ∼26 cm^3/min.

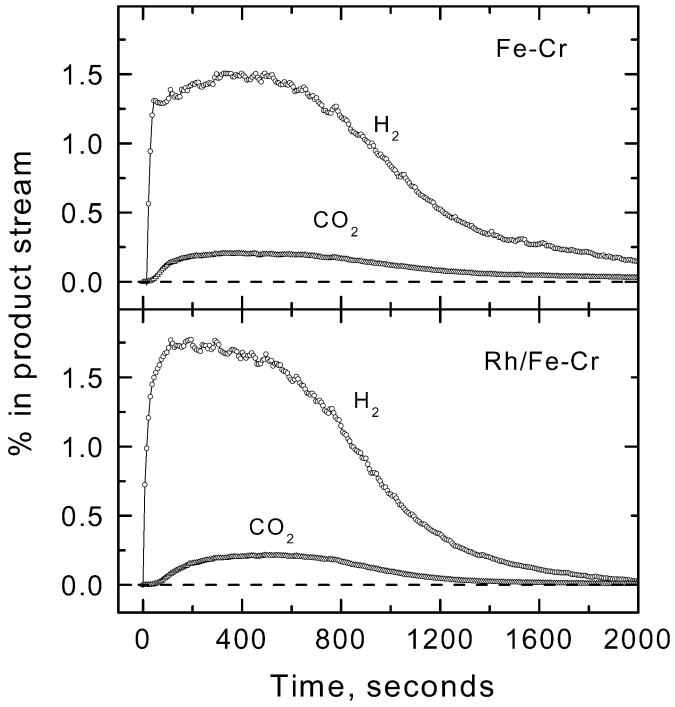

Fig. 8. Reoxidation of ∼50 mg samples of Fe–Cr and Rh/Fe–Cr, previously reduced in 7% CO/He for 1 h at 350 °C in ∼1.8% H_2O/He mixture at 380 °C. The flow rate was ∼21 cm^3/min.

any certainty when exposure times are long. Overall, Rh clearly does not noticeably promote reoxidation by CO_2.

The difference between water and carbon dioxide with respect to reoxidation of H_2-reduced samples was also apparent when a mixture of the two was used (Fig. 7). Reoxidation of the Rh-containing sample at 380 °C occurred largely with formation of H_2, whereas that of Fe–Cr was more evenly balanced between the oxidants.

Fig. 8 shows data for the reoxidation of samples in H_2O/He at 380 °C after isothermal pretreatment in 7% CO/He for 1 h at 350 °C The Fe–Cr system shows much greater H_2 evolution on treatment with water than was evident after reduction in H_2/He (Fig. 5). This reflects the greater extent of reduction possible with CO, as was also evident in the comparison TPR experiments (Figs. 2 and 3). The behavior of the Rh-promoted sample reduced in CO was similar to that of its H_2-reduced counterpart, but with a longer reaction time for the start of H_2 and a longer duration of H_2 formation. Both catalysts produced some CO_2 due to steam gasification of carbon deposited during pretreatment in CO.

Table 5 summarizes the extent to which oxygen was restored to the catalysts during the reoxidation at 380 °C illustrated in Figs. 5–8. Again the comparison is made in terms of O atoms relative to the starting Fe_2O_3. Oxygen was restored to a much greater extent for the CO reduced samples, as expected from the TPR and TPO data given in Tables 2–4.

Interpreting the data for the H_2-reduced samples is more complex, bearing in mind the thermodynamic restrictions that are apparent in Fig. 1. Bulk Fe_3O_4 cannot be easily oxidized to Fe_2O_3 by H_2O; this is feasible only when the H_2O/H_2 ratio exceeds 1.2×10^5 (at 350 °C) and cannot possibly give rise to complete conversion of water to hydrogen, as is evident at some temperatures in Figs. 5, 7, and 8. High conversions imply the presence of iron species reduced below Fe_3O_4, even though the results for TPR in hydrogen (Table 2) imply that the average stoichiometry corresponded only to that extent of reduction. There are several possible explanations for this finding. One is that the thermodynamic properties of the amorphous materials used here are very different from those tabulated for the bulk, which seems unlikely. A second possibility is that reduction in H_2/He at the temperatures used here proceeded nonuniformly with the surface reduced to a greater extent than the interior. This is a feasible explanation for the Fe–Cr system, where the extent of oxygen restoration was much less that the 0.11 ratio expected for the reversal of reaction (7). However, it is not possible to explain the results for the Rh-promoted sample in this way, because the amount of oxygen introduced was considerably greater.

Table 5
Reoxidation of previously reduced samples in H_2O and/or CO_2 at 380 °C[a]

Reduced in	H_2	H_2	H_2	CO
Reoxidised by	H_2O	CO_2	$H_2O + CO_2$	H_2O
	O atoms restored relative to those present in starting Fe_2O_3			
Fe–Cr	0.06	0.03	0.03[b], 0.03[c]	0.26 (0.03[d])
Rh/Fe–Cr	0.17	0.06	0.13[b], 0.02[c]	0.27 (0.03[d])

[a] Based on amounts generated for exposure times of 1000 s.
[b] Oxygen introduced from H_2O based on H_2 evolved.
[c] Oxygen deposited from CO_2 based on CO evolution.
[d] Carbon removed based on CO_2 evolution.

A third possible explanation is that repeated pretreatments in H_2/He, each ending with some hours at 400 °C, gave rise to a more reduced state than was achieved by a single TPR of the starting mixed oxides when carried out on a ramp ending with a shorter period at 450 °C. This interpretation seems feasible for the Rh-promoted sample, for which the generation of hydrogen atoms by spillover provided a greater driving force for reduction. According to the earlier considerations regarding the data in Fig. 1A, reduction of Fe_3O_4 to Fe is possible, but the extent to which H_2 can be utilized is quite restricted (15% conversion at most) by water formation.

3.5. Pulse reduction after the WGS reaction

These experiments were carried out using the test system used in our earlier determinations of WGS activity [8], modified with the addition of an upstream six-port valve, held at 40 °C, which enabled the introduction of 0.5-mL pulses of pure H_2 or CO into a carrier gas of Ar or He, respectively. The samples were allowed to reach steady-state WGS activity at 350 °C in a WGS feed comprising either H_2O/CO (20 and 10%, respectively in N_2) or synthetic reformate (7% CO, 8% CO_2, 22% H_2O, 37% H_2, balance N_2) and then flushed for 30 min in the carrier alone. Successive pulses of H_2 or CO were introduced at 1–2 min intervals.

The results obtained using H_2 are shown in Fig. 9. The Fe–Cr sample did not consume significant H_2 regardless of the previous exposure. The amounts consumed by the Rh/Fe–Cr sample

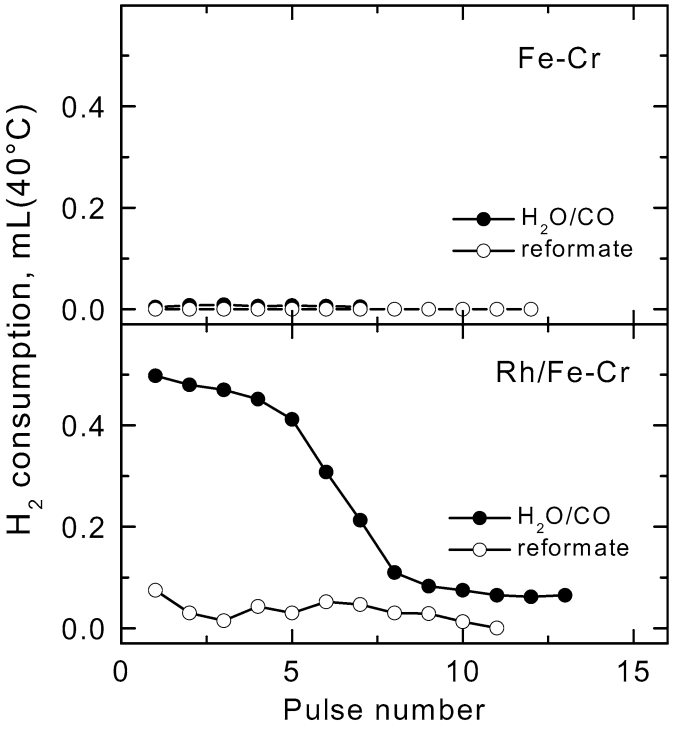

Fig. 9. Reduction of ∼50 mg samples of Fe–Cr and Rh/Fe–Cr, previously used for the water gas shift reaction with H_2O/CO and reformate feeds, at 350 °C using 0.5 mL pulses of H_2 carried in ∼30 mL/min of Ar. The points for the Fe–Cr sample exposed to H_2O/CO largely underlie those for the same sample treated in reformate.

exposed to reformate were also small, but the amounts taken up after passage of the H_2O/CO mixture were larger and showed complete consumption of H_2 for the first five pulses after equilibration. Consumption fell in subsequent pulses, leveling out at ∼15% from the tenth pulse on.

The behavior of the Rh-promoted sample can be interpreted in terms of the two lines defined by the open points in Fig. 1A that correspond to the thermodynamic reducing powers of the two feeds. The line for the reformate mixture, which largely underlies that for the ratio $H_2O/H_2 = 0.17$, is close to the Fe_3O_4-to-Fe transition line. Some reduction by reformate is conceivable bearing in mind that the thermodynamics of the amorphous oxide may differ somewhat from those of the bulk. If the outer layers are already partially reduced, then further reduction, even in pure H_2, may be difficult. On the other hand, the line for the H_2O/CO mixture lies well above the transition line, so reduction of the bulk below Fe_3O_4 is not expected while the catalyst is being used only for the WGS reaction. However, subsequent reduction to Fe in pure H_2 could be feasible, with Rh facilitating the provision of active hydrogen to drive the process.

In principle, H_2 consumption is restricted during reduction of bulk Fe_3O_4 to Fe to ∼6% at 350 °C by the H_2O/H_2 ratio allowed at equilibrium. However, this restriction is not necessarily present during pulsing if the H_2 is taken up very rapidly and water is released only slowly between pulses. It is noteworthy that the H_2 consumption does fall to a conversion much closer to the thermodynamically restricted value from the tenth pulse on. The fraction of oxygen in the sample depleted by the tenth pulse, relative to that present initially, is 0.16. Clearly the sample has been reduced well below the Fe_3O_4 expected for equilibrium with H_2O/CO feed. This confirms the inference drawn from the previously described reoxidation experiments that Rh-promoted samples used repeatedly are amenable to reduction to a lower state.

Although the thermodynamic considerations are the same for the Fe–Cr sample, this sample lacks the kinetic driving force provided by spillover from Rh and the absence of H_2 consumption after exposure to either feed is understandable.

The data for pulse reduction in CO (Fig. 10), unlike that for H_2, show significant consumption of CO (matched by the production of CO_2) regardless of the previous WGS feed. This behavior is not unexpected given the more extensive reducing power of CO. According to the thermodynamics illustrated in Fig. 1A, conversion of Fe_3O_4 to Fe at 350 °C is possible when $\ln(CO_2/CO)$ is <0.36. This would allow a CO conversion of 59% if CO and CO_2 were fully equilibrated during passage of the pulse. The consumption of CO and the production of CO_2 during the first few pulses over the Fe–Cr sample previously exposed to the H_2O/CO feed (0.3 mL out of 0.5 mL) was remarkably close to this. Consumption per pulse began to drop after the fourth pulse, consistent with the increasing difficulty of reduction with oxygen depletion from the outer layer of the catalyst, and plateaued at ∼30% per pulse.

The consumption of CO by the Rh-promoted catalyst was remarkably constant after the first pulse at ca. 45% of each pulse, regardless of pretreatment. The extent of oxygen depletion from

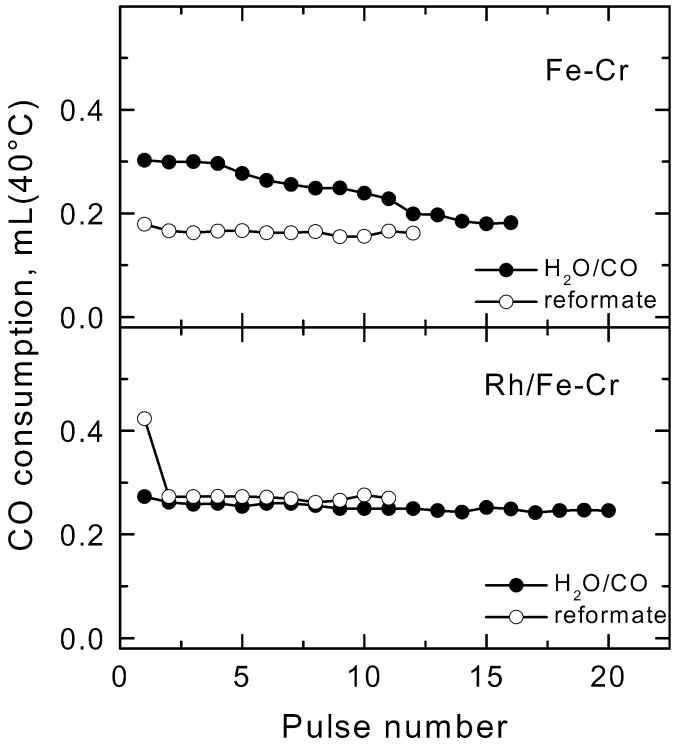

Fig. 10. Reduction of ∼50 mg samples of Fe–Cr and Rh/Fe–Cr, previously used for the water–gas shift reaction with H_2O/CO and reformate feeds, at 350 °C using 0.5 mL pulses of CO carried in ∼30 mL/min of He.

Table 6
Oxygen removal by pulse reduction at 350 °C following the WGS reaction

Pulse gas	Prior feed	Catalyst system	O atoms relative to those in starting Fe_2O_3	
			4 pulses	10 pulses
H_2	H_2O/CO[a]	Fe–Cr	0.00	–
		Rh/Fe–Cr	0.10	0.16
	Reformate[b]	Fe–Cr	–	–
		Rh/Fe–Cr	0.01	0.02
CO	H_2O/CO[a]	Fe–Cr	0.06	0.14
		Rh/Fe–Cr	0.05	0.13
	Reformate[b]	Fe–Cr	0.03	0.08
		Rh/Fe–Cr	0.06	0.15

[a] 20% H_2O, 10% CO, balance N_2.
[b] 7% CO, 8% CO_2, 22% H_2O, 37% H_2, balance N_2.

the catalyst during pulsing in H_2 and CO is summarized in Table 6. Rh was clearly important in facilitating reduction with H_2 is clear, but had little effect on reduction with CO except in the Fe–Cr system. The extent of removal by CO after 10 pulses was ∼0.14 in all cases except Fe–Cr exposed to reformate, for which it was 0.08. For the maximum number of pulses, 20 over Rh/Fe–Cr pretreated in H_2O/CO (Fig. 10), it reached 0.26 and continued. This removal was considerably greater than for H_2 reduction of the same system, which reached 0.16 after 10 pulses but exhibited a steep fall-off in consumption per pulse beyond that (Fig. 9). Clearly, pulsing CO after the WGS reaction is capable of producing greater catalyst reduction than H_2, in accordance with the earlier TPR findings.

3.6. Influence of Rh on the WGS reaction

According to the literature for iron-based catalysts [10–13], the WGS reaction can be limited by either the rate at which Fe_3O_4 is reduced by CO [step (2)] or by the rate at which H_2 is liberated during reoxidation by water [step (6)]. The results in Figs. 3 and 10 show that rhodium did not change the rates of processes involving CO, apart from the undesired deposition of carbon at temperatures above ∼360 °C. On the other hand, rhodium clearly accelerated all processes involving H_2 or H_2O (Figs. 2, 5, 7, and 9). The most telling enhancement is that of H_2 generation during reoxidation of hydrogen-reduced samples by water (Fig. 5). It is not possible to calculate the exact magnitude of this enhancement. The extent of reduction before reoxidation was not the same for the two catalysts, and the H_2 liberation process is likely to differ as well from direct generation from hydroxyl groups for the Fe–Cr catalyst versus surface migration of H atoms, reverse spillover, and recombination when Rh is present. However, it is apparent from Fig. 5 that the rhodium-containing catalyst was more effective at 280 °C than the unpromoted catalyst at 380 °C. For an activation energy of 63 kJ/mol, as observed for the WGS reaction over the Rh-promoted catalyst [9], this difference in temperature is equivalent to a factor of >8 in rate. This is more than sufficient to account for the measured differences in WGS activity in Table 1, and hence it is highly likely that rhodium acts by accelerating the rate of step (6) rather than of step (2).

4. Conclusion

Rhodium promotion of the high-temperature WGS reaction on iron/chromium oxide catalysts is matched by substantial increases in the rates of particular reduction/oxidation steps. This enhancement is evident in each process related to the H_2/H_2O couple: reduction of the starting material from the Fe_2O_3 form and generation of H_2 from water during reoxidation of repeatedly reduced samples and during pulse reduction with H_2 after use in a H_2O/CO WGS feed. As expected, on thermodynamic grounds, CO can achieve a greater extent of reduction in matched tests, and reduction by CO may also proceed at lower temperatures than reduction by H_2, but no steps in the CO/CO_2 couple are promoted by rhodium. Rhodium promotion of the H_2/H_2O couple is consistent with enhancement of the rates of dissociation of hydrogen molecules and recombination of hydrogen atoms on the metal, together with hydrogen atom transfer between metal and oxide by forward/reverse spillover. It is highly likely that facilitation of the latter processes is the origin of rhodium promotion of the WGS reaction.

Acknowledgments

This work was supported by grants from the Australian Research Council. The authors are grateful to Macquarie University for the loan of key equipment used in the step-change and TPR experiments.

References

[1] D.L. Trimm, Z.I. Onsan, Catal. Rev.-Sci. Eng. 43 (2001) 31.
[2] D.L. Trimm, Appl. Catal. A: Gen. 296 (2005) 1.
[3] W. Ruettinger, O. Ilinich, R.J. Farrauto, J. Power Sources 118 (2003) 61.
[4] X. Liu, W. Ruettinger, X. Xu, R. Farrauto, Appl. Catal. B 2005 (2005) 69.
[5] Q. Fu, W. Deng, H. Saltsburg, M. Flytzani-Stephanopoulos, Appl. Catal. B 56 (2005) 57.
[6] M.V.E. Twigg, Catalyst Handbook, Wolfe Scientific, London, 1989.
[7] C. Rhodes, B.P. Williams, F. King, G.J. Hutchings, Catal. Commun. 3 (2002) 381.
[8] Y. Lei, N.W. Cant, D.L. Trimm, Catal. Lett. 103 (2005) 133.
[9] Y. Lei, N.W. Cant, D.L. Trimm, Chem. Eng. J. 114 (2005) 81.
[10] R.L. Keiski, T. Salmi, P. Niemesto, J. Ainassaari, V.J. Pohjola, Appl. Catal. A: Gen. 137 (1996) 349.
[11] S. Oki, R. Mezaki, J. Phys. Chem. 77 (1973) 1601.
[12] M. Tinkle, J.A. Dumesic, J. Catal. 103 (1987) 65.
[13] S. Oki, R. Mezaki, Ind. Eng. Chem. Res. 27 (1988) 15.
[14] G.C. Chinchen, R.H. Logan, M.S. Spencer, Appl. Catal. 12 (1984) 89.
[15] M.A. Edwards, D.M. Whittle, C. Rhodes, A.M. Ward, D. Rohan, M.D. Shannon, G.J. Hutchings, C.J. Kiely, Phys. Chem. Chem. Phys. 4 (2002) 3902.
[16] B.N. Kuznetsov, M.G. Chidinov, A.M. Alekseev, V.I. Yakerson, Kinet. Catal. 37 (1996) 908.
[17] S. Stolen, R. Glockner, F. Gronvold, Thermochim. Acta 256 (1995) 91.
[18] H. Liu, X. Li, Ind. Eng. Chem. Res. 36 (1997) 335.
[19] B. Herzog, D. Herein, R. Schlogl, Appl. Catal. A: Gen. 141 (1996) 71.
[20] G. Ketteler, W. Weiss, W. Ranke, R. Schlogl, Phys. Chem. Chem. Phys. 3 (2001) 1114.
[21] W.K. Jozwiak, T.P. Maniecki, A. Basinska, J. Goralski, R. Fiederow, Kinet. Catal. 45 (2004) 930.
[22] X. Li, Y. Cen, H. Liu, Y. Xu, G. Lv, React. Kinet. Catal. Lett. 81 (2004) 313.
[23] I. Barin, Thermochemical Data of Pure Substances, VCH, Weinheim, 1989.